Quantum Electronics **44** (12) 1085–1090 (2014)

INTERACTION OF LASER RADIATION WITH MATTER. LASER PLASMA

PACS numbers: 42.65.Jx; 42.65.Re; 52.38.Hb
DOI: 10.1070/QE2014v044n12ABEH015472

Plasma channels during filamentation of a femtosecond laser pulse with wavefront astigmatism in air

A.A. Dergachev, A.A. Ionin, V.P. Kandidov, D.V. Mokrousova, L.V. Seleznev, D.V. Sinitsyn, E.S. Sunchugasheva, S.A. Shlenov, A.P. Shustikova

Abstract. **We have demonstrated experimentally and numerically the possibility of controlling parameters of plasma channels formed during filamentation of a femtosecond laser pulse by introducing astigmatism in the laser beam wavefront. It is found that weak astigmatism increases the length of the plasma channel in comparison with the case of aberration-free focusing and that strong astigmatism can cause splitting of the plasma channel into two channels located one after another on the filament axis.**

Keywords: *filamentation, femtosecond laser pulse, laser plasma, laser filament.*

1. Introduction

Propagation of high-power femtosecond laser pulses in media with cubic nonlinearity leads to the development of beam self-focusing and to an increase in radiation intensity. Self-focusing and filamentation develop in the case when the laser pulse peak power exceeds the critical power of self-focusing, P_{cr}, in a medium. In air, the latter varies, according to different estimates, from 2 to 6 GW at a wavelength of 800 nm and is equal to about 70 MW at 248 nm. The collapse of the beam is limited by the free-electron plasma generated in a high-power laser field. Dynamic balance of focusing cubic (Kerr) nonlinearity and defocusing plasma nonlinearity causes the formation of a stable extended structure of radiation, i.e., a filament, which is accompanied by the formation of a plasma channel [1, 2].

Plasma channels formed during laser filamentation can be used to produce waveguide systems [3–5] and to control electrical discharges [6, 7]. For such plasma channels to be used in practice, one must be able to control their position, length and concentration of electrons in these channels. Increasing filament and plasma channel lengths with pulse phase modulation was investigated theoretically in [8] and experimentally (on an extended atmospheric path) in [9]. However, apart from the length, phase modulation strongly influences the longitudinal position and structure of the channel, which splits into individual plasma bunches in the case of strong modulation. Geints et al. [10] controlled the position of the plasma channel onset by various aperture diaphragms. The use of a circular aperture led to an almost twofold increase in the length of the region of multiple filamentation [11]. Axicon focusing of the beam can suppress multiple filamentation of a femtosecond pulse and result in an extended plasma channel, which cannot be done by lens focusing [12]. One of the drawbacks of the above methods is a significant loss of pulse energy on a limiting aperture or during the formation of diffraction rings after it passes through an axicon. An interesting approach was used by Ionin et al. [13], where the channel length was increased without pulse energy loss by distorting the beam wavefront (additional spherical aberration was introduced into the beam) with a relatively expensive deformable mirror.

In this paper, we propose a simple method for controlling parameters of plasma channels of femtosecond filaments without energy loss, namely, by introducing astigmatism in the laser beam. It should be noted that in previous work [14] the effect of astigmatism on ordering of multiple filamentation was studied. Here we investigate the influence of astigmatism on filamentation in the regime of a single filament.

2. Experiment

The experiments were performed using a Ti:sapphire laser system [10, 13] from the Gas Lasers Laboratory at the P.N. Lebedev Physics Institute, RAS. The centre wavelength was 744 nm and the pulse duration was about 100 fs (FWHM). Pulse energy in these experiments was varied from 1 to 3.5 mJ and pulse peak power exceeded the critical power of self-focusing in air, P_{cr}. The beam radius at the $1/e^2$ level was 3 mm. Filamentation of a laser pulse was carried out in the regime of a single filament.

The scheme of the experiment is shown in Fig. 1. IR laser radiation was focused by a spherical mirror with a focal length f_0. In the case of close-to-normal incidence of laser radiation, focusing can be considered aberration-free with a parabolic wavefront

$$\varphi(x,y) = \frac{k(x^2+y^2)}{2f_0}, \tag{1}$$

where $k = 2\pi/\lambda$. If the mirror is rotated so that the incident and reflected beams form an angle α, then there appear wavefront aberrations $\varphi(x,y)$ in the form of astigmatism:

A.A. Dergachev, V.P. Kandidov, S.A. Shlenov Department of Physics and International Laser Center, M.V. Lomonosov Moscow State University, Vororb'evy gory, 119991 Moscow, Russia;
e-mail: dergachev88@yandex.ru;
A.A. Ionin, D.V. Mokrousova, L.V. Seleznev, D.V. Sinitsyn, E.S. Sunchugasheva, A.P. Shustikova P.N. Lebedev Physics Institute, Russian Academy of Sciences, Leninsky prosp. 53, 119991 Moscow, Russia;

Received 21 March 2014; revision received 27 June 2014
Kvantovaya Elektronika **44** (12) 1085–1090 (2014)
Translated by I.A. Ulitkin

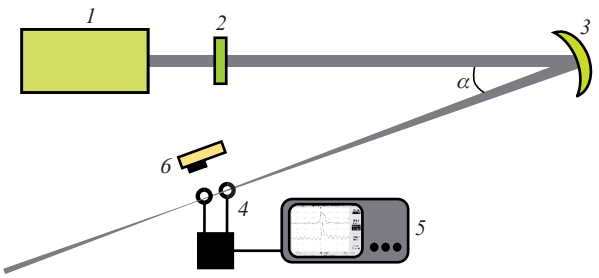

Figure 1. Scheme of the experiment: (*1*) Ti:sapphire laser; (*2*) diffraction attenuator; (*3*) spherical mirror; (*4*) electrodes; (*5*) oscilloscope; (*6*) CCD camera.

$$\varphi(x,y) = \frac{kx^2}{2f_x} + \frac{ky^2}{2f_y}. \qquad (2)$$

As a dimensionless parameter characterising astigmatism, we will use the quantity $\Delta f/f_0$, equal to the ratio of the distance between the tangential (f_x) and sagittal (f_y) foci (longitudinal measure) $\Delta f = |f_x - f_y|$ to the average focal length $f_0 = (f_x + f_y)/2$. If astigmatism is not too strong, one can expect the entire region between the two foci of the beam to form a waist with a sufficiently high peak intensity of light, and this should lead to the formation of a longer (as compared to aberration-free focusing) plasma channel. In the case of stronger astigmatism one can expect the channel to split into two regions located near the geometric foci of the beam. In the experiments the angle α was increased up to 45°. Figure 2 shows the dependence of the position of the beam foci f_x and f_y and the astigmatism parameter $\Delta f/f_0$ on the angle between the beams, α, calculated in the geometrical optics approximation.

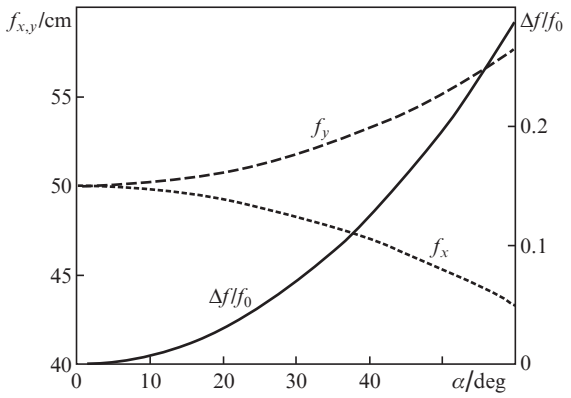

Figure 2. Dependences of the positions f_x and f_y of the tangential and sagittal foci of an astigmatic beam and dimensionless astigmatism parameter $\Delta f/f_0$ on the angle α between the incident and reflected beams at the focal length of the mirror $f_0 = 50$ cm.

To register a plasma channel in the experiments with different focusing mirrors ($f_0 = 25$, 52 and 110 cm), we used a longitudinal electrostatic scheme (Fig. 1). The laser pulse in this case propagated through small holes in two parallel electrodes in the form of flat disks 25 mm in diameter. The interelectrode spacing was 5 mm and the voltage between the electrodes was 300 V. The change of conductivity of the space between the electrodes resulted in appearance of a current which was recorded with an oscilloscope. By moving the measuring system along the optical axis we measured the plasma density (in relative units) along the plasma channel.

Figure 3 shows the images of the plasma channels obtained experimentally for a laser pulse with an energy of 3.5 mJ, whose power is almost ten times higher than P_{cr}. In these experiments, the CCD camera was located near the region of filamentation, from one side of the plasma channel (Fig. 1). In the case of normal incidence of laser radiation (Fig. 3a) the plasma channel was formed in front of the geometrical focus and passed through it. Increasing angle of incidence (an increase in the astigmatism parameter $\Delta f/f_0$) led to the formation of two plasma segments. Even at relatively small ($\alpha \approx 20°$) angles ($\Delta f/f_0 \approx 0.03$, Fig. 3b) we observed the appearance of the second peak in the longitudinal distribution of the plasma density. With increasing astigmatism the first channel located near the tangential focus was shifted towards the laser beam and the second channel ended far beyond the focus (Figs 3b–d). The length of the first plasma channel decreased with increasing astigmatism. Thus, by varying the astigmatism parameters, one can control the plasma channel length and position.

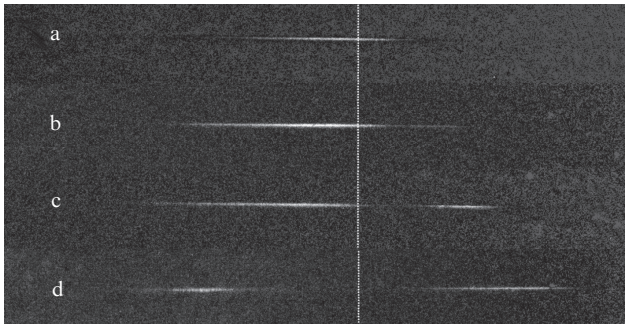

Figure 3. Images of plasma channels obtained by the CCD camera at the astigmatism parameter $\Delta f/f_0$ = (a) 0, (b) 0.03, (c) 0.05 and (d) 0.16. The laser pulse energy is 3.5 mJ. The longitudinal dimension of the region presented is 9 cm. The pulse falls from left to right. The vertical line corresponds to the focal plane of the mirror ($f_0 = 25$ cm).

Figure 4 shows the distributions of the plasma density along the plasma channels produced upon different laser beam focusing. The angle α in these experiments was 15° ($\Delta f/f_0 \approx 0.017$) and 45° ($\Delta f/f_0 = 0.16$). In the case of tight focusing, an increase in the astigmatism parameter led to the formation of two distinct peaks in the plasma channel (Fig. 4a). It is interesting to note that when there were two such peaks in the distribution of the plasma density along the channel, the amplitude of the first peak (along the pulse path) was smaller than that of the second one (Figs 4a–c). A similar behaviour was observed at less tight focusing ($f_0 = 52$ cm) in the case of a lower-energy laser pulse (1.1 mJ, Fig. 4b). At $f_0 = 52$ cm an increase in energy by almost half (to 1.7 mJ) resulted in the merging of the plasma segments near the geometrical focus of the beam, which was accompanied by the formation of a single plasma channel (Fig. 4c). Thus, the length of the plasma channel increased slightly with increasing astigmatism parameter as compared with the case of aberration-free focusing. In the case of less tight focusing ($f_0 = 110$ cm) a change in astigmatism virtually had no effect on the length of the plasma channel (Fig. 4d). Thus, the increase in astigmatism caused a decrease in plasma density (see Fig. 7 below). It should be noted that by increasing the tightness of focusing the maxi-

mum plasma density in plasma channels increased, resulting in a higher amplitude of the detected signal. Thus, in the case of strong astigmatism, a decrease in the laser pulse energy and/or an increase in the focusing tightness result in the lengthening of the plasma channel in comparison with the case of aberration-free pulse propagation and to the appearance of two peaks in the distribution of the plasma density along the channel.

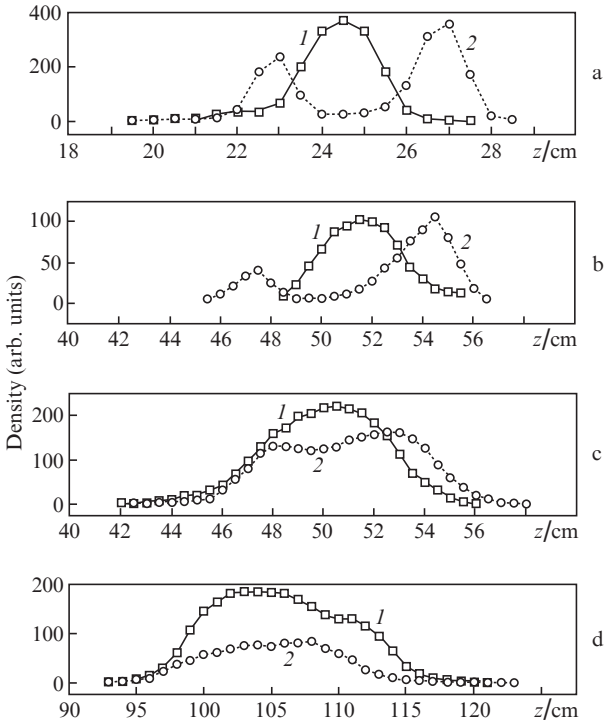

Figure 4. Distributions of the linear plasma density along the plasma channels at f_0 = (a) 25, (b, c) 52 and (d) 110 cm. The pulse energy is (a, c, d) 1.7 and (b) 1.1 mJ. The astigmatism parameter is $\Delta f/f_0 \approx 0.017$ and ~0.16 at the angles α = (*1*) 15° and (*2*) 45°, respectively, between the incident and reflected beams.

3. Numerical simulation

The propagation of a high-power femtosecond laser pulse in a nonlinear medium is described by the system of equations for the slowly varying complex amplitude of the light field, $A(x,y,z,\tau)$, and the concentration of free electrons, $n_e(x,y,z,\tau)$ [15]. In the retarded coordinate system, these equations have the form

$$2ik_0\frac{\partial A}{\partial z} = \frac{\partial^2 A}{\partial x^2} + \frac{\partial^2 A}{\partial y^2} + 2k_0\tilde{D}A + \frac{2k_0^2}{n_0} \times(\Delta n_K + \Delta n_{pl})A - ik_0A\delta, \quad (3)$$

$$\Delta n_K(x,y,z,\tau) = \frac{1}{2}n_2I(x,y,z,\tau) + \frac{1}{2}\int_{-\infty}^{\tau} n_2I(x,y,z,t')H(\tau-t')\,dt', \quad (4)$$

$$\Delta n_{pl}(x,y,z,\tau) = -\frac{2\pi e^2}{m_e n_0 \omega_0^2}n_e(x,y,z,\tau), \quad n_e = n_e^{(1)} + n_e^{(2)}, \quad (5)$$

$$\frac{\partial n_e^{(1,2)}}{\partial \tau} = R^{(1,2)}(I)(n^{(1,2)0} - n_e^{(1,2)}), \quad (6)$$

where $\tau = t - zn_0/c$; n_0 is the refractive index at the centre wavelength λ_0; $k_0 = 2\pi/\lambda_0$; $\omega_0 = 2\pi c/\lambda_0$; and e and m are the electron charge and mass. The first two terms on the right hand side of equation (3) for the complex field amplitude describe diffraction in the parabolic approximation and the operator $\tilde{D}$ – dispersion of laser radiation in the medium, which was accounted for in the spectral space. In this case, the dispersion of air for the wavelength in question is given by the relation

$$n(\lambda) = 1 + C\left(1 + \frac{B}{\lambda^2}\right) \quad (7)$$

with the parameters $C = 2.879 \times 10^{-4}$ and $B = 5.67 \times 10^{-11}$ cm^2 [16]. The expression for the Kerr nonlinearity (4) took into account both an instantaneous and a delayed response, caused by the scattering on rotational transitions of the molecules of the air medium [17]. The response function (4) was approximated by the expression [18]

$$H(\tau) = \Omega^2\exp\left(-\frac{\Gamma\tau}{2}\right)\frac{\sin\Lambda\tau}{\Lambda}$$

with the parameters Ω = 20.6 THz, Γ = 26 THz and $\Lambda = \sqrt{\Omega^2 - \Gamma^2/4}$. The critical power of self-focusing $P_{cr} = 3.77\lambda^2 \times (8\pi n_0 n_2)^{-1}$ in the calculations was ~2 GW at λ_0 = 744 nm and 70 MW at λ_0 = 248 nm [19, 20].

The dynamics of the electron concentration $n_e^{(1,2)}$ in equation (6) at times of the order of the pulse duration is determined by the ionisation rates $R^{(1,2)}$ of oxygen (superscript 1) and nitrogen (superscript 2) molecules, which depend on the light field intensity I, and by the initial concentrations of these molecules, $n^{(1)0}$ and $n^{(2)0}$. For laser radiation at λ_0 = 744 nm the ionisation rates $R^{(1,2)}$ were calculated using the Popov–Perelomov–Terentyev model [21]. For UV pulses over the entire range of intensities, applicable is the multiphoton approximation, according to which

$$R^{(1,2)}(I) = \sigma^{(1,2)}I^{K^{(1,2)}}, \quad (8)$$

where $K^{(1,2)}$ are the minimum numbers of photons at the central frequency, the total energy of which exceeds the ionisation energy of the molecules, $W^{(1,2)}$; and $\sigma^{(1,2)}$ are the cross sections of photoionisation processes: $\sigma^{(1)} = 1.34 \times 10^{-27}$ cm^6 s^{-1} W^{-3} and $\sigma^{(2)} = 2.4 \times 10^{-43}$ cm^8 s^{-1} W^{-4} [22–24].

The coefficient δ in (3) takes into account energy losses due to ionisation of the medium.

We considered laser radiation with a Gaussian pulse shape and a Gaussian beam profile:

$$A(x,y,z=0,\tau) = A_0\exp\left(-\frac{x^2+y^2}{2r_0^2}\right) \times\exp\left(-\frac{\tau^2}{2\tau_0^2}\right)\exp[i\varphi(x,y)], \quad (9)$$

where $\varphi(x,y)$ is the phase modulation (2).

According to the results of numerical simulations performed on 'Chebyshev' and 'Lomonosov' supercomputers at the Moscow State University Research Computing Center [25] we calculated the fluence

$$F(x,y,z) = \int_{-\infty}^{\infty} I(x,y,z,\tau)\,\mathrm{d}\tau,$$

linear plasma density

$$\rho_{\mathrm{lin}}(z) = \int_{0}^{\infty} n_{\mathrm{e}}(x,y,z,\tau = +\infty)\,\mathrm{d}x\mathrm{d}y$$

and the total number of free electrons

$$Q_{\mathrm{e}}^{\mathrm{total}} = \int_{0}^{L} \rho_{\mathrm{lin}}(z)\,\mathrm{d}z,$$

formed by the pulse propagating over the distance L.

4. Calculation results and discussion

We simulated numerically the formation of plasma channels in the case of filamentation of laser radiation with the parameters close to experimental ones and various longitudinal astigmatism parameters. The pulse duration was 100 fs and its energy was 1.1 mJ, corresponding to the peak power $5P_{\mathrm{cr}}$. The beam radius was $r_0 = 3$ mm and the average focal length was $f_0 = 50$ cm. The astigmatism parameter varied from zero (aberration-free focusing) to 0.16.

Figure 5 shows the distributions of the linear electron concentration ρ_{lin} along the filament for IR and UV pulses. An increase in the astigmatism parameter first leads to the formation of a more extended channel and then to a break of a single channel into two regions in the vicinity of the tangential (front, with a greater concentration of electrons) and sagittal (rear) foci. The results obtained experimentally for the focal length $f_0 = 50$ cm and in numerical simulations are shown in Fig. 6 for weak and strong astigmatism. The parameter $\Delta f/f_0$ is equal to 0.017 and 0.16, which corresponds to the angles of 15° and 45° between the beams incident on and reflected from the mirror. Comparison of the experimental results and the results of numerical simulations shows that they are in qualitative agreement with each other; in particular, the numerical simulation well reproduces the experimentally observed separation of the plasma channel into two channels with increasing astigmatism.

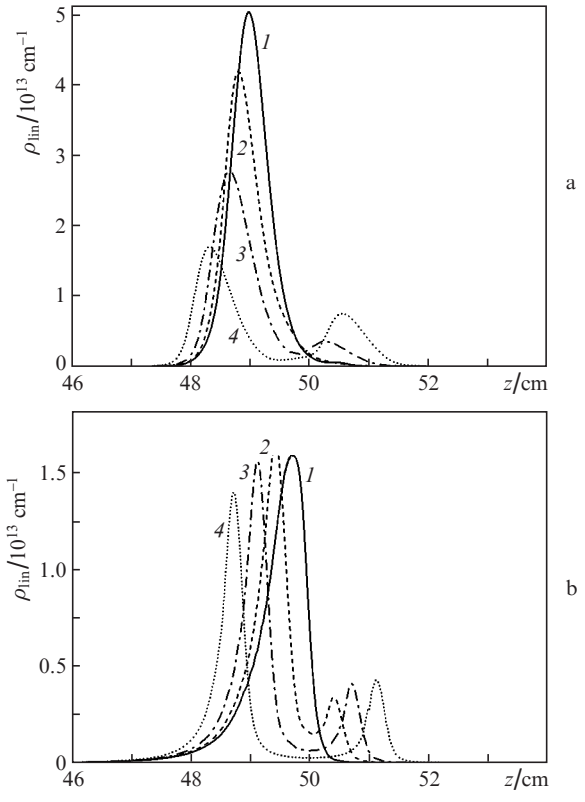

Figure 5. Linear concentration of electrons in plasma channels of (a) IR and (b) UV pulses at the astigmatism parameter $\Delta f/f_0$ = (*1*) 0, (*2*) 0.017, (*3*) 0.03 and (*4*) 0.048.

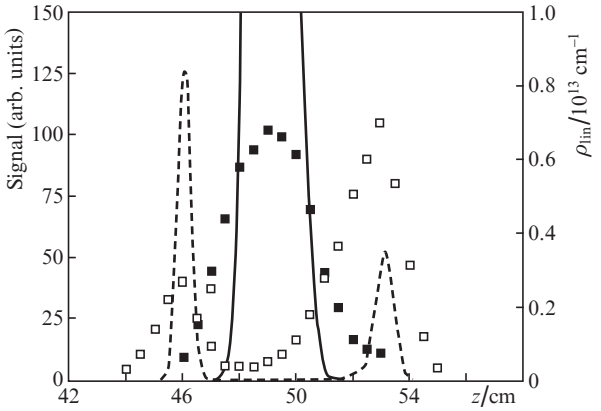

Figure 6. Change in the signal measured in the experiment (points) and numerically obtained distribution of the linear electron concentration ρ_{lin} (curves) along the direction z of the IR pulse propagation at $\Delta f/f_0$ = 0.017, α = 15° (■, solid curve) and $\Delta f/f_0$ = 0.16, α = 45° (□, dashed curve).

It should be noted that a relative decrease in the maximum values of the linear electron concentration with increasing astigmatism parameter in the calculation was significantly higher than that measured experimentally. One reason for this may be the limitations of the model used in the calculation, which does not take into account nonlinear perturbations of the pulse parameters in solid-state laser system elements. These perturbations can lead to additional dynamic (changing during the pulse) beam wavefront aberrations in the case of both weak and strong astigmatism, thereby smoothing out the difference in the peak values of the pulse intensity and the density of the plasma generated by it. Another possible reason may be the relaxation of the plasma during the recording of the signal in the experiment, which is not included in the numerical model.

Figure 7 shows the dependences of the peak intensity I in the filament and maximum linear electron concentration ρ_{lin} in plasma channels of IR and UV pulses as well as the total number $Q_{\mathrm{e}}^{\mathrm{total}}$ of free electrons for both wavelengths on the astigmatism parameter. One can see that an increase in wavefront astigmatism of the beam leads to a monotonic decrease in the peak intensity in the filament (almost twice in this range of parameters). This is due to the fact that in the case of strong astigmatism the geometric focusing actually occurs first only along one of the two transverse directions (for example along the x axis), which prevents the rapid formation of a nonlinear focus. The character of focusing becomes similar to that of slit beam focusing, and to prevent the collapse it suffices to use an optically weaker diverging lens formed by self-induced

plasma in the filament channel. The decrease in intensity in the filament causes a sharp decrease in the ionisation rate, and thus the concentration of electrons in the laser plasma is greatly reduced. However, as shown by the results of numerical simulations, the diameter of the plasma channels of IR radiation at the e^{-1} level does not change or slightly decreases. This eventually leads to a reduction in the total number of electrons by approximately 50 times (Fig. 7c and Fig. 4d). UV pulses are characterised by an increase in the diameter of plasma channels; therefore, the linear plasma density decreases slowly (Fig. 7b) and the total number of electrons in the plasma channel decreases only by 3.5 times (Fig. 7c).

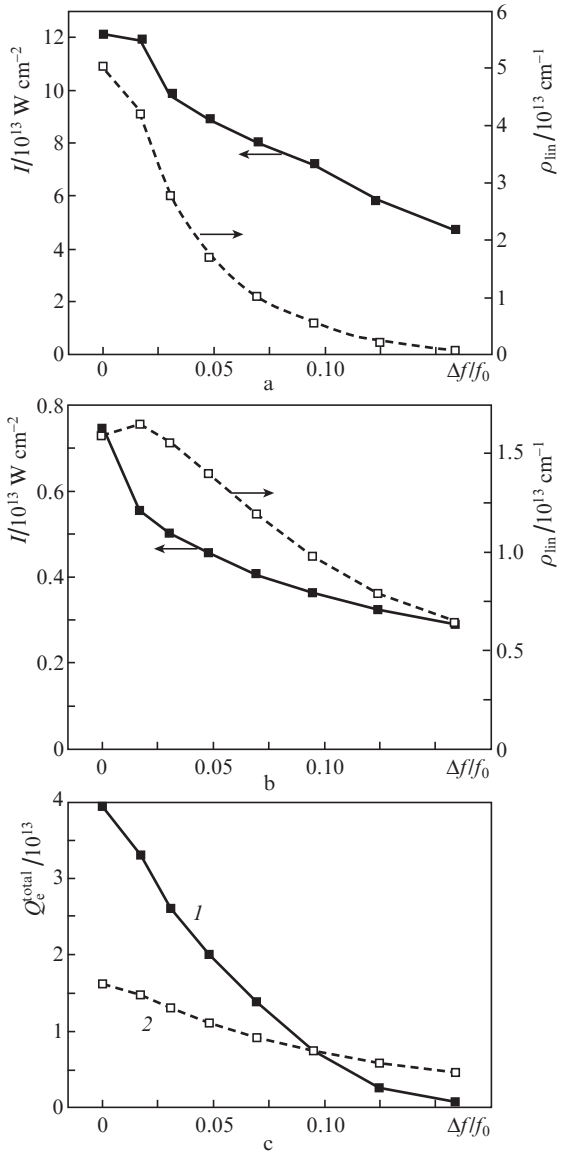

Figure 7. Peak intensity I in the filament and linear electron concentration ρ_{lin} in the plasma channel during filamentation of (a) IR and (b) UV radiation with wavefront astigmatism of the beam and (c) the total number Q_e^{total} of electrons in the plasma channels of (*1*) IR and (*2*) UV pulses.

Thus, the introduction of wavefront astigmatism in the beam leads to an increase in the length of the channel as compared with the case of the aberration-free beam focusing, wherein the plasma channel can extend beyond the sagittal focus of the beam. When astigmatism is further increased, two channels are formed near the tangential and sagittal foci.

To find the dependence of the parameters of the plasma channels of the laser beams with wavefront astigmatism on their radius r_0, we performed the numerical simulation for $r_0 = 1$ and 2.5 mm, while maintaining a constant peak beam power ($P_0 = 5P_{cr}$). The positions of the tangential and sagittal beam foci remained fixed (80 and 100 cm, respectively, and $\Delta f/f_0 = 0.22$). Under these conditions, an increase in the beam radius results in tighter focusing in the presence of astigmatism. As a result, the peak values of the linear plasma density along the path varied from 2.3×10^{12} cm^{-1} at $r_0 = 1$ mm to 2.3×10^{10} cm^{-1} at $r_0 = 2.5$ mm.

When the beam radius is small ($r_0 = 1$ mm), the regime of weak focusing is realised, accompanied by the formation of a plasma channel that is uniform in the longitudinal direction. At the onset of this regime one can observe a sharp increase in the linear plasma density and then its gradual decrease (Fig. 8). When the beam radius is large ($r_0 = 2.5$ mm), both waists near the tangential and sagittal foci are short and do not overlap each other. As a result, two longitudinally spaced plasma channel regions are formed: a region with a greater linear plasma density in the vicinity of the front focus and a more extended (but with a lower density) region in front of the rear focus. Thus, upon weak focusing the splitting of the plasma channel into two may not be observed even when astigmatism is sufficiently strong.

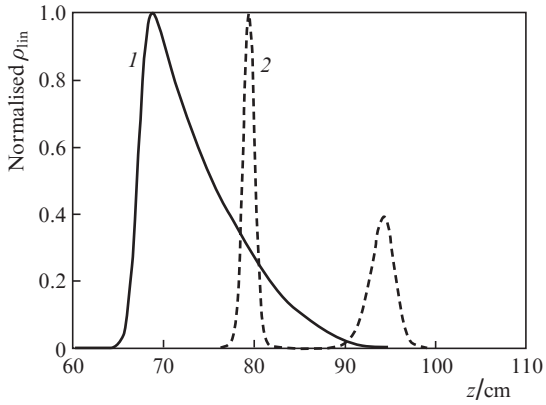

Figure 8. Normalised linear electron density in the plasma channels of IR pulse filaments at the beam radii $r_0 =$ (*1*) 1 and (*2*) 2.5 mm. Front and rear beam foci are located at a distance $z = 80$ and 100 cm, respectively.

5. Conclusions

We have studied the formation of plasma channels by IR and UV femtosecond laser pulses with wavefront astigmatism of the beam. We have found numerically and experimentally that weak astigmatism increases the length of the plasma channel in comparison with the case of aberration-free focusing and strong astigmatism can cause the formation of two channels following each other on the filament axis. It is shown that weaker focusing and/or an increase in energy of the beam with astigmatism result in the merging of the plasma channels. Thus, the introduction of wavefront astigmatism of a femtosecond laser beam allows one to control the position and length of the plasma channels in the filament without any power loss.

Acknowledgements. This work was supported by the Russian Foundation for Basic Research (Grant Nos 14-02-00489 and 14-22-02021-ofi-m), the RF President's Grant Council (State Support to Leading Scientific Schools Programme, Grant No. NSh-3796.2014.2) and the Educational-Scientific Complex of the Lebedev Physics Institute.

References

1. Couairon A., Mysyrowicz A. *Phys. Rep*., **441**, 47 (2007).
2. Kandidov V.P., Shlenov S.A., Kosareva O.G. *Kvantovaya Elektron*., **39**, 205 (2009) [*Quantum Electron*., **39**, 205 (2009)].
3. Schwarz J., Rambo P., Giuggioli L., Diels J.-C. *Proc. OSA/NLGW* (Clearwater, Fl, 2001) 467/WC6.
4. Dormidonov A.E., Valuev V.V., Dmitriev V.L., Shlenov S.A., Kandidov V.P. *Proc. SPIE Int. Soc. Opt. Eng*., **6733**, 67332S (2007).
5. Valuev V.V., Dormidonov A.E., Kandidov V.P., Shlenov S.A., Kornienko V.N., Cherepenin V.A. *Raditekh Elektron*., **55** (2), 222 (2010).
6. La Fontaine B., Comtois D., Chien C.-Y., Desparois A., Gérin F., Jarry G., Johnston T., Kieffer J.-C., Martin F., Mawassi R., Pépin H., Rizk F.A.M., Vidal F., Potvin C., Couture P., Mercure H.P. *J. Appl. Phys*., **88**, 610 (2000).
7. Tzortzakis S., Prade B.S., Franco M.A., Mysyrowicz A., Huller S., Mora P. *Phys. Rev. E*, **64**, 057401 (2001).
8. Golubtsov I.S., Kandidov V.P., Kosareva O.G. *Kvantovaya Elektron*., **33**, 525 (2003) [*Quantum Electron*., **33**, 525 (2003)].
9. Mechain G., d'Amico C., Andre Y.B., Tzortzakis S., Franco M., Prade B., Mysyrowicz A., Couairon A., Salmon E., Sauerbrey R. *Opt. Commun*., **247**, 171 (2005).
10. Geints Yu.E., Zemlyanov A.A., Izyumov N.A., Ionin A.A., Kudryashov S.I., Seleznev L.V., Sinitsyn D.V., Sunchugasheva E.S. *Zh. Eksp. Teor. Fiz*., **143**, 228 (2013).
11. Daigle J.-F., Kosareva O.G., Panov N.A., Begin M., Lessard F., Marceau C., Kamali Y., Roy G., Kandidov V.P., Chin S.L. *Appl. Phys. B*, **94**, 249 (2009).
12. Kosareva O.G., Grigor'evskii A.V., Kandidov V.P. *Kvantovaya Elektron*., **35**, 1013 (2005) [*Quantum Electron*., **35**, 1013 (2005)].
13. Ionin A.A., Iroshnikov N.G., Kosareva O.G., Larichev A.V., Mokrousova D.V., Panov N.A., Seleznev L.V., Sinitsyn D.V., Sunchugasheva E.S. *J. Opt. Soc. Am. B*, **30**, 2257 (2013).
14. Mechain G., Couairon A., Franco M., Prade B., Mysyrowicz A. *Phys. Rev. Lett*., **93**, 035003 (2004).
15. Dergachev A.A., Ionin A.A., Kandidov V.P., Seleznev L.V., Sinitsyn D.V., Sunchugasheva E.S., Shlenov S.A. *Kvantovaya Elektron*., **43**, 29 (2013) [*Quantum Electron*., **43**, 29 (2013)].
16. Born M., Wolf E. *Principles of Optics* (London: Pergamon, 1970; Moscow: Nauka, 1973).
17. Oleinikov P.A., Platonenko V.T. *Laser Phys*., **3**, 618 (1993).
18. Mlejnek M., Wright E.M., Moloney J.V. *Opt. Lett*., **23**, 382 (1998).
19. Loriot V., Hertz E., Faucher O., Lavorel B. *Opt. Express*, **17**, 13429 (2005).
20. Shaw M.J., Hooker C.J., Wilson D.C. *Opt. Commun*., **103**, 153 (1993).
21. Perelomov A.M., Popov V.S., Terentyev M.V. *Zh. Eksp. Teor. Fiz*., **50**, 1393 (1966) [*Sov. Phys. JETP*, **23**, 924 (1966)].
22. Schwarz J., Rambo P., Diels J.-C., Kolesik M., Wright E.M., Moloney J.V. *Opt. Commun*., **180**, 383 (2000).
23. Tzortzakis S., Lamouroux B., Chiron A., Moustaizis S.D., Anglos D., Franco M., Prade B., Mysyrowicz A. *Opt. Commun*., **197**, 131 (2001).
24. Couairon A., Tzortzakis S., Bergé L., Franco M., Prade B., Mysyrowicz A. *J. Opt. Soc. Am. B*, **19**, 1117 (2002).
25. Dergachev A.A., Silaeva E.P., Shlenov S.A., in *Superkomp'yutenye tekhnologii v nauke, obrazovanii i promyshlennosti* (Supercomputer Technologies in Science, Education and Industry) (Moscow: Izd-vo MGU, 2010) p. 100.